Supporting Information

A Metal-Assembled, Resorcin[4]arene-Based Molecular Trimer for Efficient Removal of Toxic Dichromate Pollutant and Knoevenagel Condensation Reaction

Xue Han,[†] Ya-Xin Xu,[†] Jin Yang,*[,†] Xianxiu Xu,[‡] Cheng-Peng Li,*[,§] and Jian-Fang Ma*[,†]

[†]*Key Lab for Polyoxometalate Science, Department of Chemistry, Northeast Normal University, Changchun 130024, China.*

[‡]*College of Chemistry, Chemical Engineering and Materials Science, Key Laboratory of Molecular and Nano Probes, Ministry of Education, Shandong Normal University, Jinan 250014, China.*

[§]*College of Chemistry, Tianjin Key Laboratory of Structure and Performance for Functional Molecules, MOE Key Laboratory of Inorganic-Organic Hybrid Functional Material Chemistry, Tianjin Normal University Tianjin 300387, China.*

* Correspondence authors

E-mail: yangj808@nenu.edu.cn (J. Yang)

E-mail: hxxylcp@tjnu.edu.cn (C.-P. Li)

E-mail: majf247@nenu.edu.cn (J.-F. Ma)

Fax: +86-431-85098620 (J.-F. Ma)

Experimental Section

Material and Methods. All chemicals were commercially available. The tetrakis(1,2,4-triazol-ylmethyl)resorcin[4]arene (TTR4A) was prepared by following the literature method.[1] FT-IR spectrum was determined on a Mattson Alpha Centauri spectrometer. PXRD pattern was performed on a Rigaku Dmax 2000 X-ray diffractometer with graphite monochromatized CuK_{α} radiation (λ = 0.154 nm). Elemental analytic data was conducted on a Euro vector EA3000 elemental analyzer. Thermogravimetric curves were measured on a Perkin-Elmer Model TG-7 analyzer.

X-Ray Crystallography. Crystallographic data of **1-NO_3** was collected on an Oxford Diffraction Gemini R Ultra diffractometer using graphite-monochromated MoKα radiation (λ = 0.71073 Å). The structure was solved by the direct methods with SHELXS-2014, and refined by full-matrix least-squares technique using the SHELXL-2014 within WINGX.[2-4] The multi-scan method was applied for absorption corrections. Non-hydrogen atom was refined anisotropically. The SQUEEZE function in PLATON was employed to remove the residual electron density.[5] Crystallographic data was listed in Table S2. Selected bond lengths and angles were afforded in Table S3.

Synthesis of $[Cd_3(TTR4A)_3(H_2O)_6]\cdot 6NO_3\cdot 3DMF\cdot 3H_2O$ (1-NO_3). A mixture of TTR4A (10 mg, 0.01 mmol), $Cd(NO_3)_2\cdot 4H_2O$ (12 mg, 0.04 mmol), isonicotinic acid (6 mg, 0.04 mmol), DMF (3 mL) and water (3 mL) was sealed in a 10 mL glass vial and heated at 80 °C for three days. After cooling to room temperature, colorless crystals were obtained in 16% yield. Anal. Calcd for $C_{153}H_{171}O_{54}N_{45}Cd_3$ (*Mr* = 3841.54): C, 47.84; H, 4.49; N, 16.41. Found: C, 46.98; H, 4.58; N, 16.55. IR data (KBr, cm^{-1}): 3438 (W), 3119 (W), 2673 (w), 1662 (m), 1595 (m), 1516 (m), 1469 (s), 1384 (m), 1276 (m), 1097 (s), 1061 (s), 1017 (s), 642 (m), 574 (m), 501 (m).

Sample Activation. Crystalline sample of **1-NO_3** was immersed in acetone for three days before Knoevenagel condensation reaction. After filtration, the exchanged sample was activated at 90 °C under vacuum for 10 h. Upon activation, the diffraction peaks of the PXRD pattern became greatly weak. When the activated sample was

further soaked in the mother liquor, the PXRD pattern can be restored, demonstrating that the structure was still maintained after activation.

Procedure for Anion Exchange. 1-NO_3 (30 mg) was immersed in an aqueous solution (5 mL) of $K_2Cr_2O_7$ (3 mM, 5 mM and 7 mM) and the resulting mixture was static at room temperature. The anion exchange process was monitored by UV/Vis spectroscopy based on the typical sorption of $Cr_2O_7^{2-}$ at 353 nm.

Anion Selectivity Study. Crystalline sample of **1-NO_3** (10 mg) was immersed in an aqueous solution (3 mL) of $K_2Cr_2O_7$ (5 mM), to which the NO_3^- and $H_2PO_4^-$ (5 mM/200 mM) were added. After 24 h, the solution was monitored by UV/Vis absorption spectroscopy at room temperature.

Knoevenagel Condensation Reaction. Crystalline sample of **1-NO_3** (0.003 mmol) was added to the mixture of benzaldehyde derivative (1 mmol) and malononitrile (2 mmol) in a 15 mL round-bottom flask. Then the mixture was stirred at 60 °C for 1 h. The conversion yield of the substrate was analyzed by GC and ^{1}H NMR with tridecane as internal standard.

(1) Hu, Y.-J.; Yang, J.; Liu, Y.-Y.; Song, S.; Ma, J.-F. A Family of Capsule-Based Coordination Polymers Constructed from a New Tetrakis(1,2,4-triazol-ylmethyl)resorcin[4]arene Cavitand and Varied Dicarboxylates for Selective Metal-Ion Exchange and Luminescent Properties. *Cryst. Growth Des.* **2015**, *15*, 3822-3831.

(2) Sheldrick, G. M. SHELXS-2014, Program for The Crystal Structure Solution; University of Göttingen: Göttingen, Germany, **2014**.

(3) Sheldrick, G. M. SHELXL-2014, Program for The Crystal Structure Refinement; University of Göttingen: Göttingen, Germany, **2014**.

(4) Farrugia, L. J. WINGX: A Windows Program for Crystal Structure Analysis; University of Glasgow: Glasgow, U.K., **1988**.

(5) Spek, A. L. PLATON SQUEEZE: A Tool for The Calculation of The Disordered Solvent Contribution to The Calculated Structure Factors. *Acta Crystallogr. Sect. C: Struct. Chem*. **2015**, *71*, 9-18.

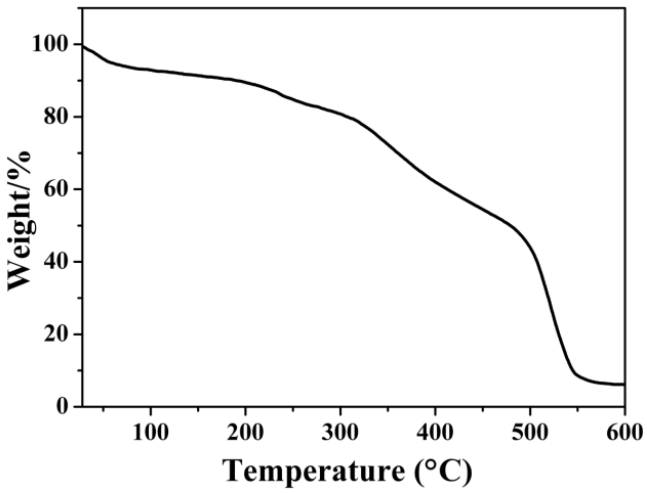

Figure S1. TG curves of the **1-NO$_3$**. The weight loss corresponding to the release of three DMF and nine water molecules was observed before 193 °C for **1-NO$_3$** (obsd: 89.9%, calcd: 90.0%).

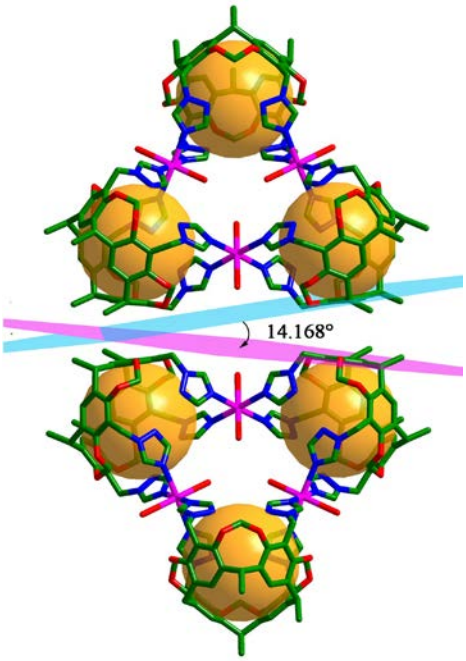

Figure S2. The dihedral angle between two phenyl rings for the aromatic π-π interaction.

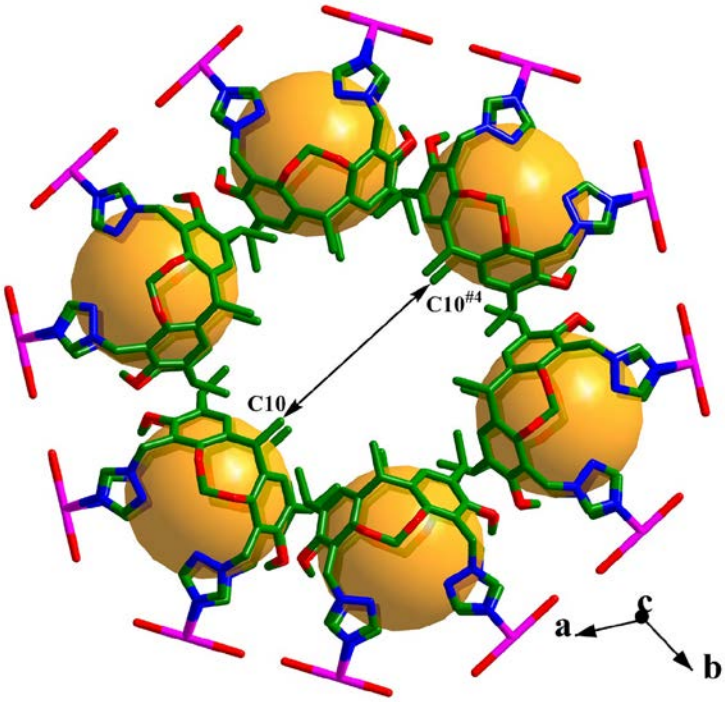

Figure S3. The channel diameter based on C10 and its symmetry-related $C10^{\#4}$ atoms regardless of the van der Waals radius. Symmetry code: $^{\#4}$ 1+*x*-*y*, 2-*y*, 1-*z*.

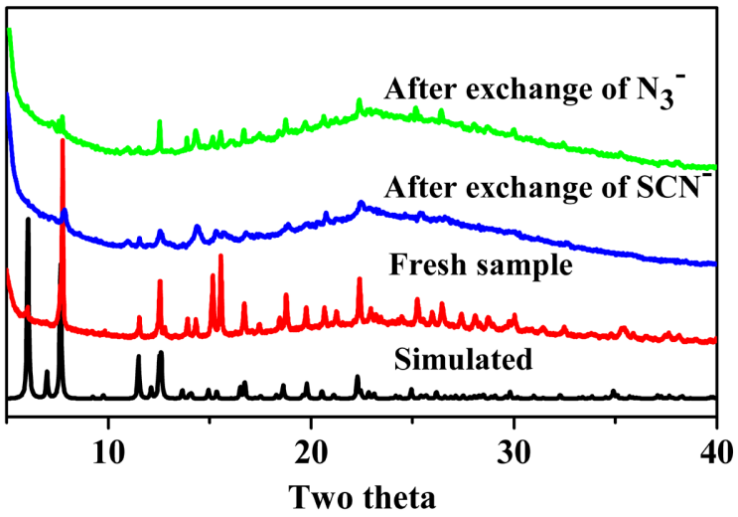

Figure S4. PXRD patterns of the simulated (black), the experimental (red) and after exchange of SCN^- (blue) and N_3^- (green).

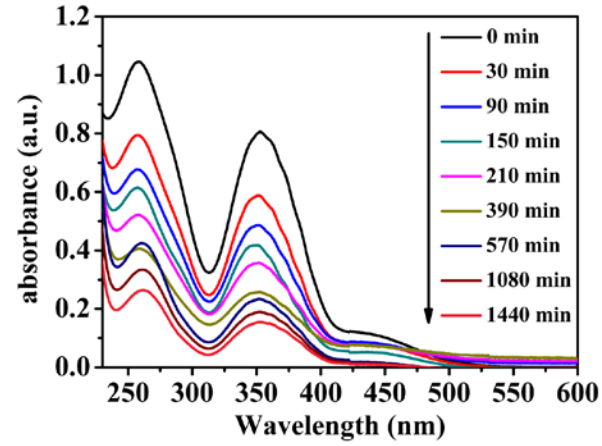

(a)

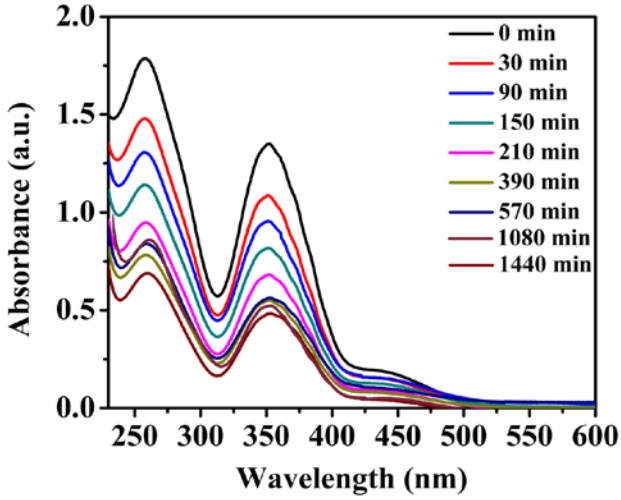

(b)

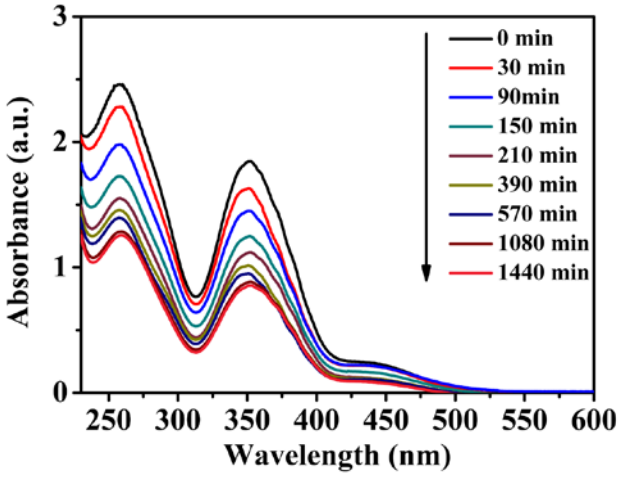

(c)

Figure S5. Uv-vis adsorption spectra of dichromate exchange with different concentrations of **1-NO_3**: 3 mM (a), 5 mM (b) and 7 mM (c).

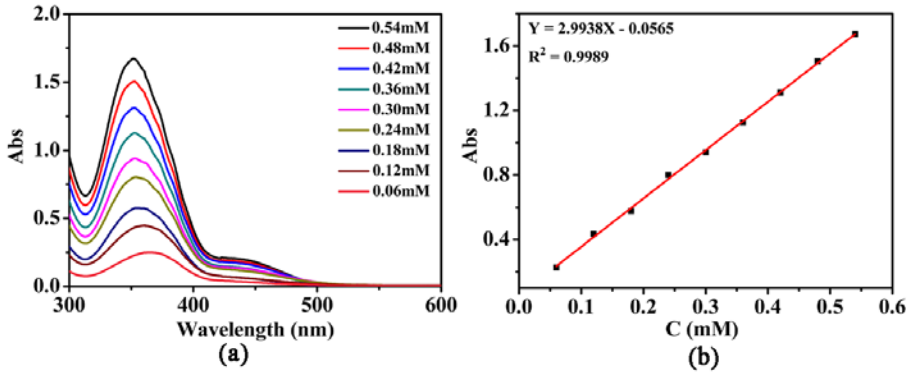

Figure S6. (a) Calibration plot of standard $Cr_2O_7^{2-}$ determined by UV/vis spectra in aqueous solution. (b) The fitting of concentration of $Cr_2O_7^{2-}$ *vs* Abs value.

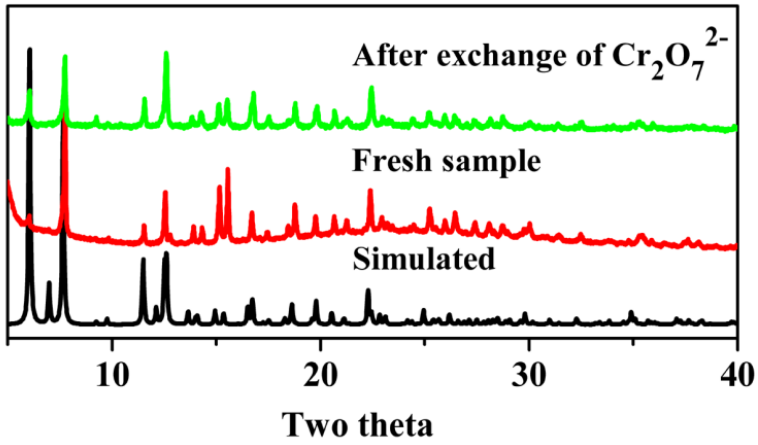

Figure S7. PXRD patterns of the simulated (black), the experimental (red) and after exchange of $Cr_2O_7^{2-}$ (green).

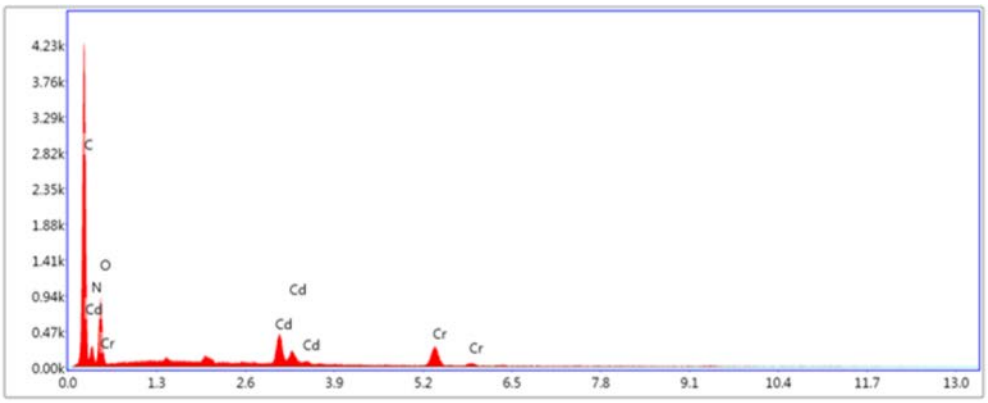

Figure S8. EDX spectrum for **1-Cr_2O_7**.

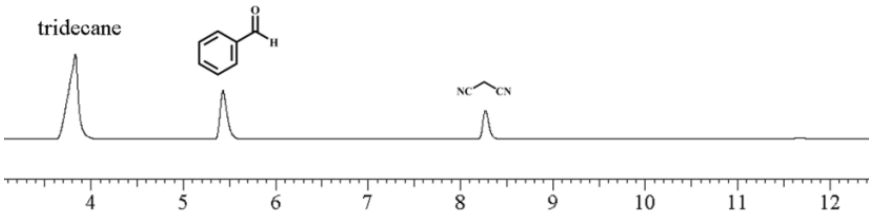
tridecane
4 5 6 7 8 9 10 11 12

(a)

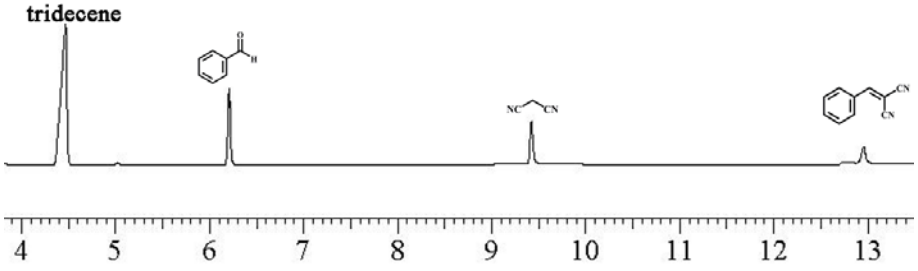
tridecene
4 5 6 7 8 9 10 11 12 13

(b)

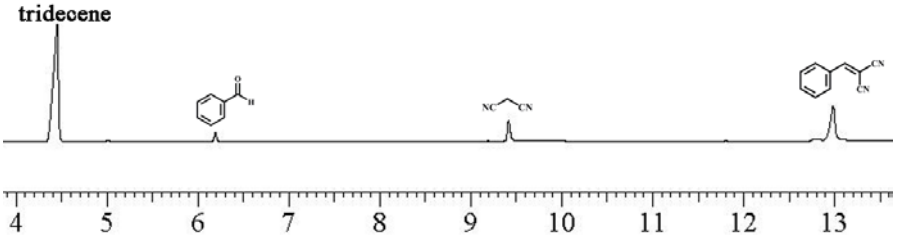
tridecene
4 5 6 7 8 9 10 11 12 13

(c)

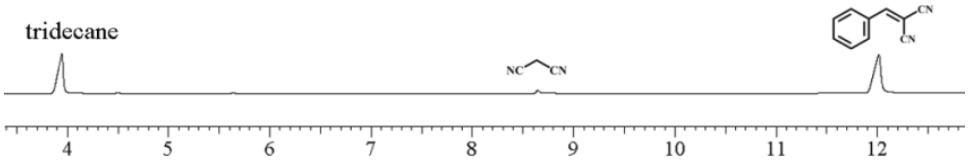
tridecane
4 5 6 7 8 9 10 11 12

(d)

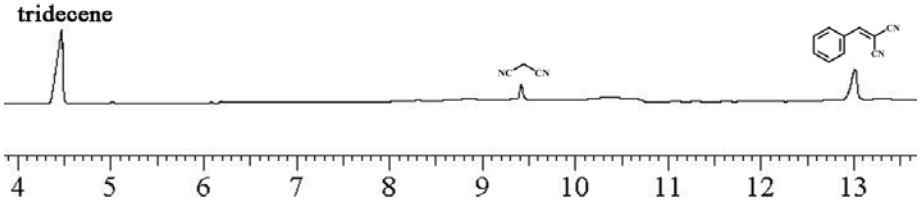
tridecene
4 5 6 7 8 9 10 11 12 13

(e)

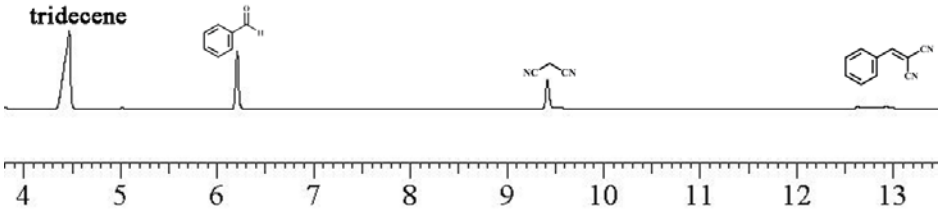
tridecene
4 5 6 7 8 9 10 11 12 13

(f)

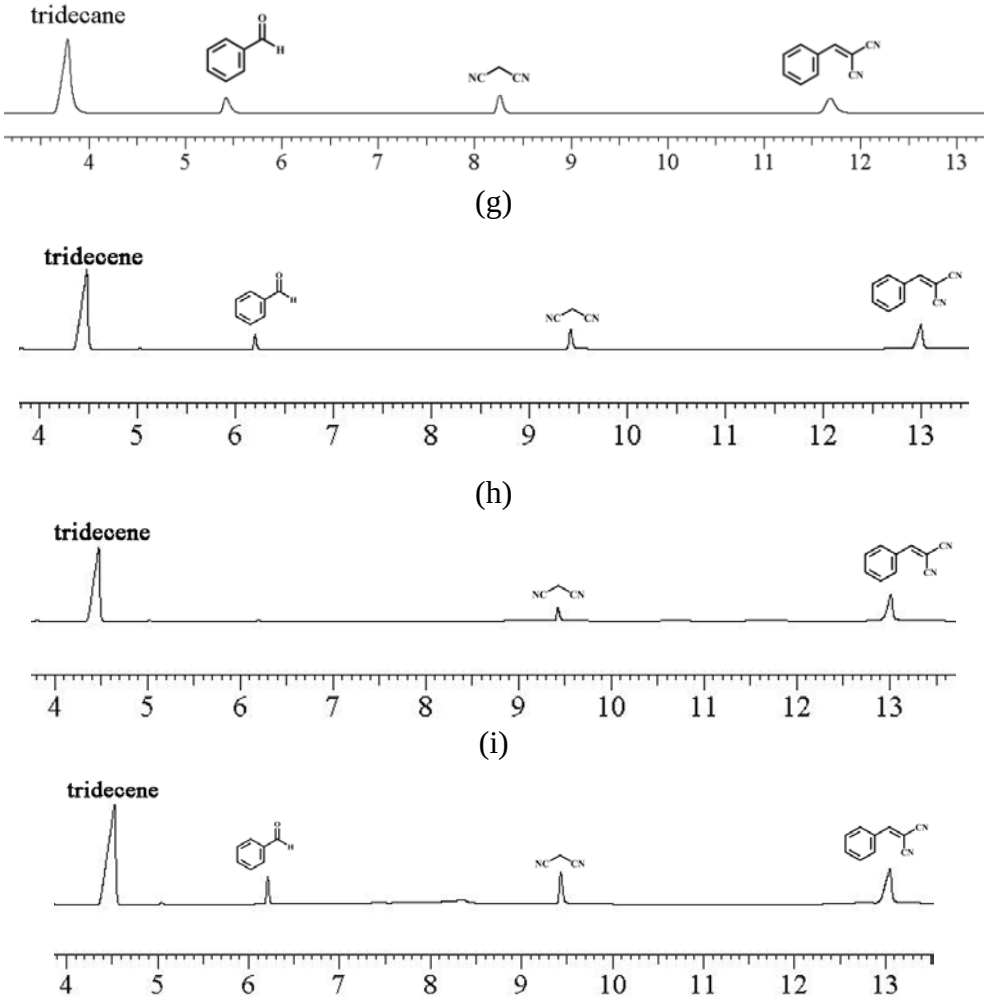

(g)

(h)

(i)

(j)

Figure S9. GC of Knoevenagel condensation reaction of malononitrile with benzaldehyde: (a) without catalyst after catalytic reaction of 1 h at 60 °C; (b-e) with 0.001, 0.0002, 0.003 and 0.004 mmol catalyst **1-NO_3** after 1 h at 60 °C, respectively; (f-i) using **1-NO_3** as catalyst after 1 h at 30 °C, 40°C, 50°C and 70°C, respectively; (j) with TTR4A as catalyst after 1 h at 60 °C.

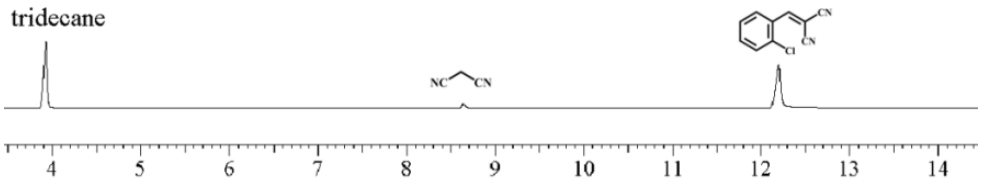

(a)

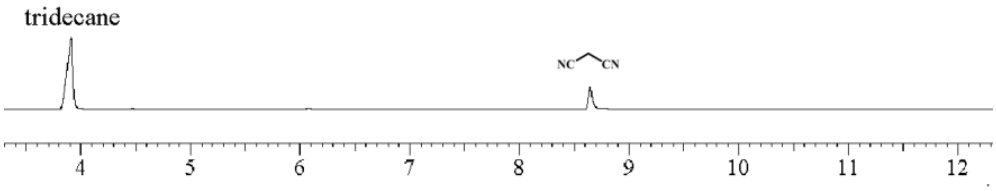
tridecane
NC CN
4 5 6 7 8 9 10 11 12

(b)

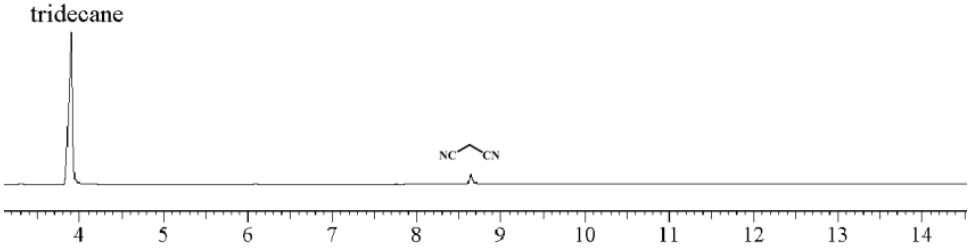
tridecane
NC CN
4 5 6 7 8 9 10 11 12 13 14

(c)

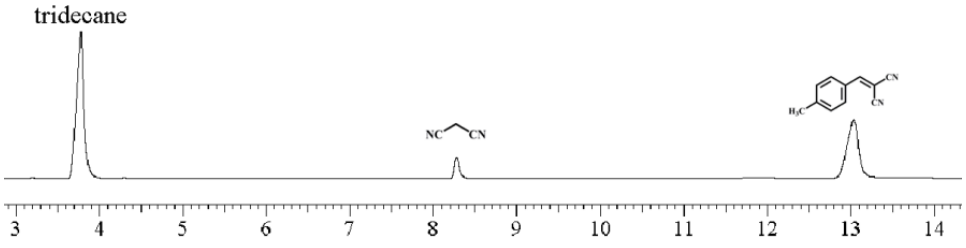
tridecane
NC CN
3 4 5 6 7 8 9 10 11 12 13 14

(d)

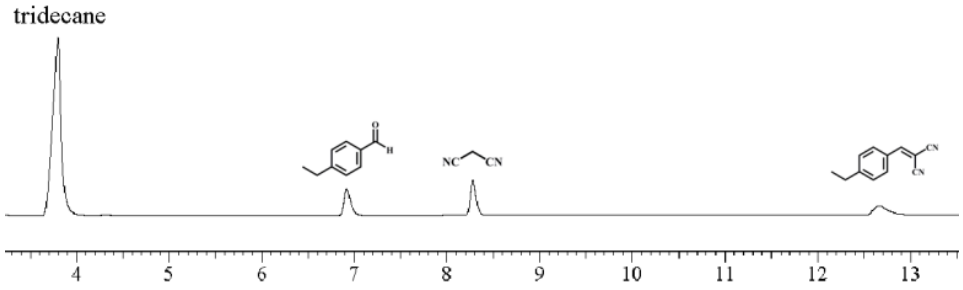
tridecane
NC CN
4 5 6 7 8 9 10 11 12 13

(e)

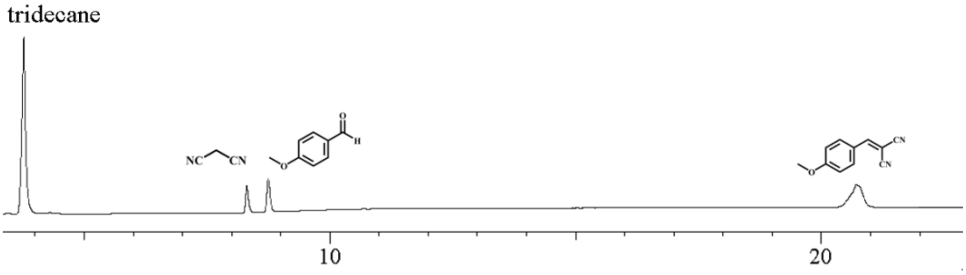
tridecane
NC CN
10 20

(f)

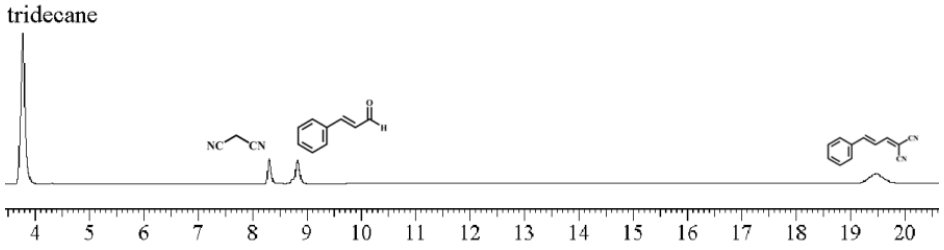

(g)

Figure S10. GC of Knoevenagel condensation reaction of malononitrile with benzaldehyde: (a)-(g) GC of Knoevenagel condensation reaction of malononitrile with benzaldehyde derivatives using **1-NO_3** as catalyst after 1 h at 60 °C.

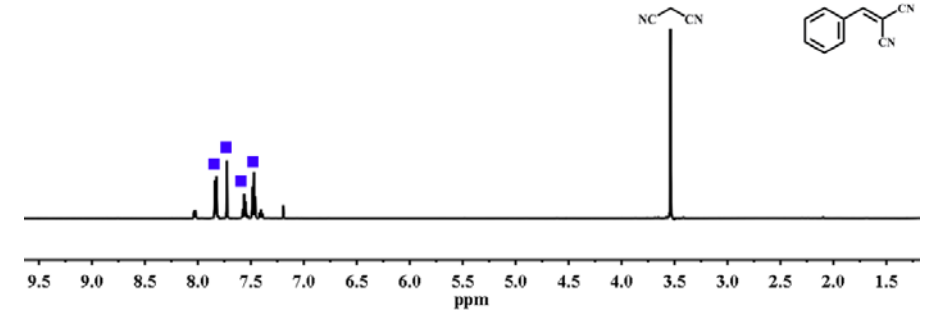

(a)

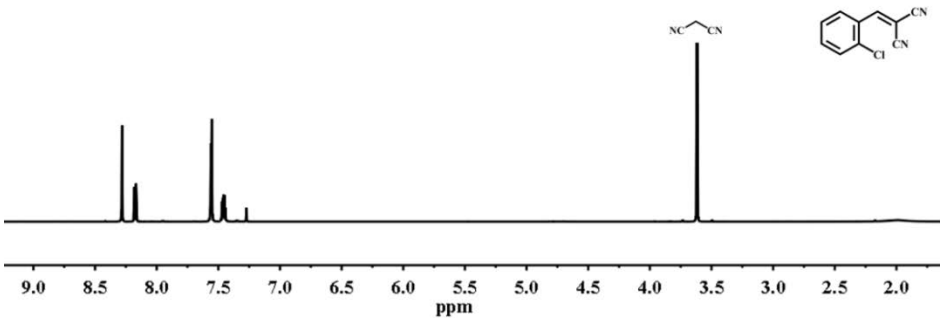

(b)

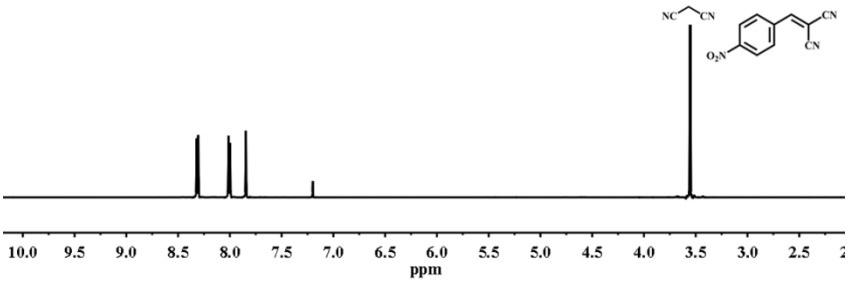

(c)

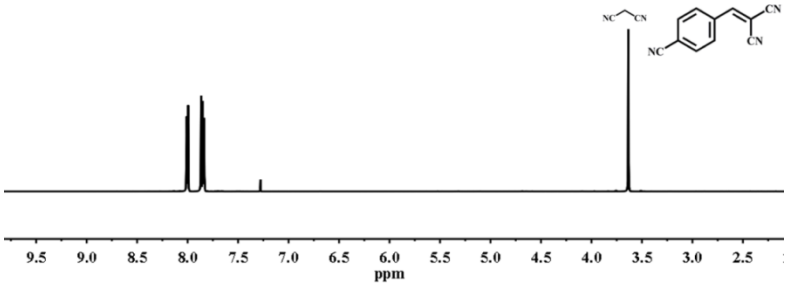
9.5 9.0 8.5 8.0 7.5 7.0 6.5 6.0 5.5 5.0 4.5 4.0 3.5 3.0 2.5
ppm

(d)

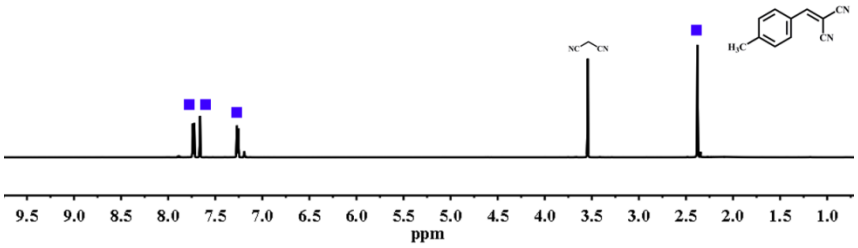
9.5 9.0 8.5 8.0 7.5 7.0 6.5 6.0 5.5 5.0 4.5 4.0 3.5 3.0 2.5 2.0 1.5 1.0
ppm

(e)

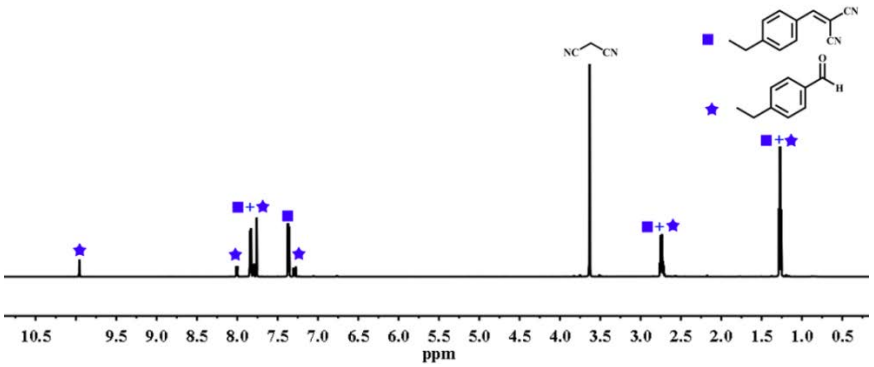
10.5 9.5 9.0 8.5 8.0 7.5 7.0 6.5 6.0 5.5 5.0 4.5 4.0 3.5 3.0 2.5 2.0 1.5 1.0 0.5
ppm

(f)

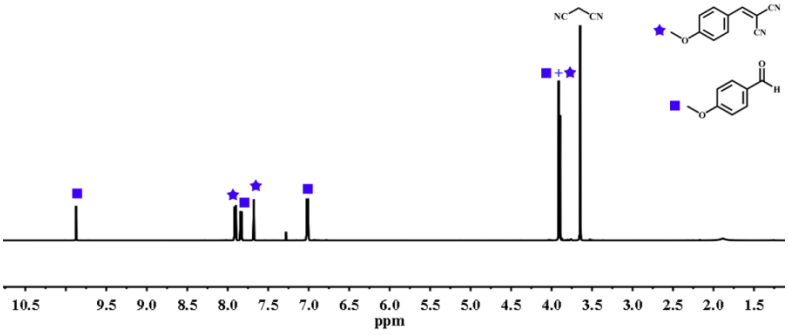
10.5 9.5 9.0 8.5 8.0 7.5 7.0 6.5 6.0 5.5 5.0 4.5 4.0 3.5 3.0 2.5 2.0 1.5
ppm

(g)

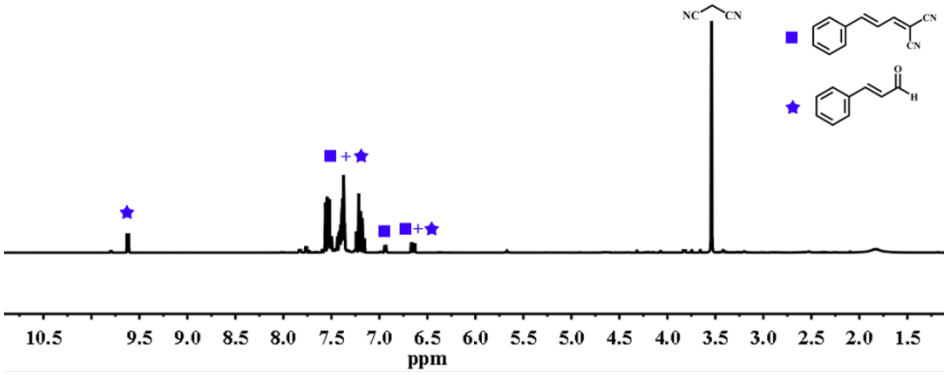

(h)

Figure S11. ^{1}H NMR spectra of the products from the Knoevenagel condensation reactions of the malononitrile with different benzaldehyde derivatives using **1** as catalyst: (a) using benzaldehyde as substrate; (b) using 2-chlorobenzaldehyde as substrate; (c) using 4-nitrobenzaldehyde as substrate; (d) using 4-cyanobenzaldehyde as substrate; (e) using 4-methylbenzaldehyde as substrate; (f) using 4-ethylbenzaldehyde as substrate; (g) using 4-methoxybenzaldehyde as substrate; (h) using cinnamaldehyde as substrate.

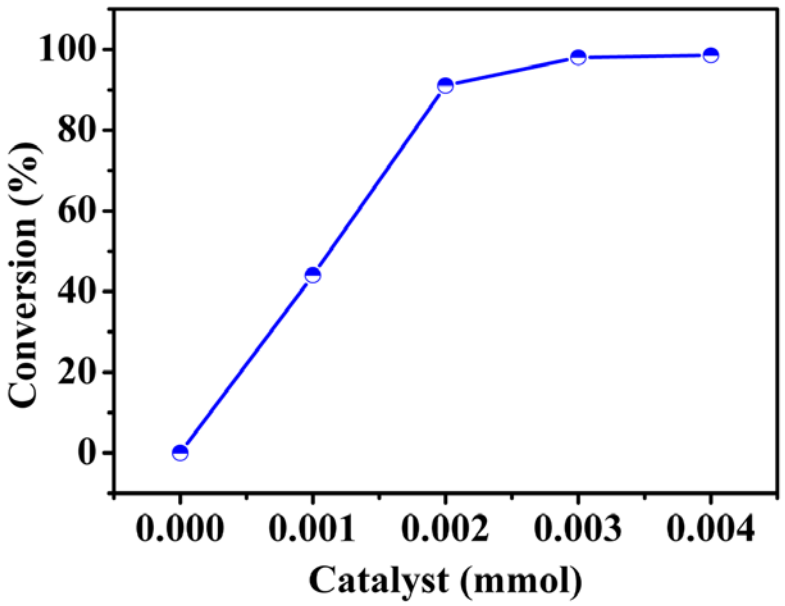

Figure S12. Conversions of the benzaldehyde with catalyst amount in Knoevenagel condensation reaction at 60 °C for 1 h.

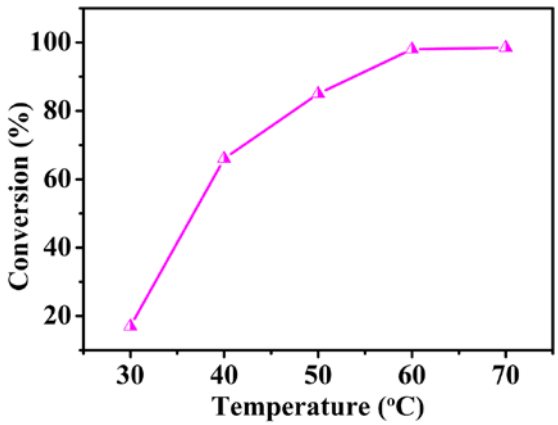

Figure S13. Conversions of the benzaldehyde with temperatures in Knoevenagel condensation reaction using **1-NO$_3$** as catalyst (0.003 mmol) for 1 h.

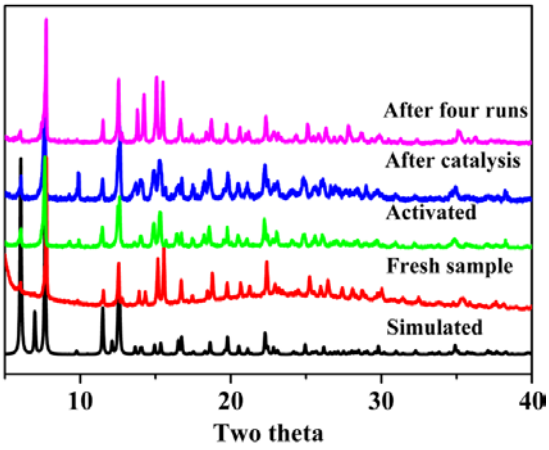

Figure S14. PXRD patterns of the simulated (black), the experimental (red), after activated (blue), after catalysis (green) and after four runs (pink).

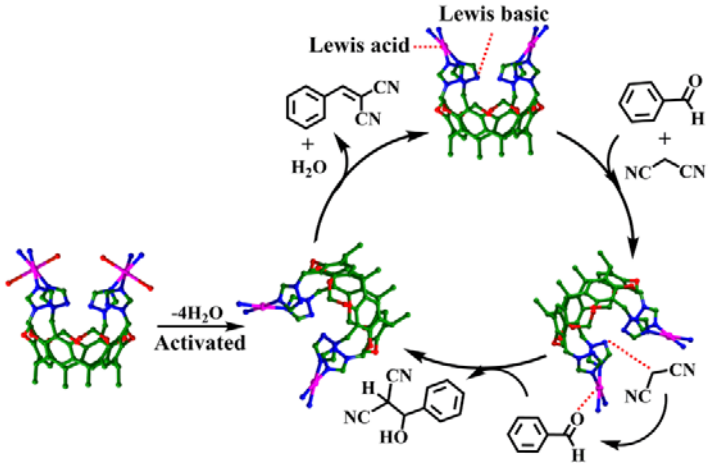

Figure S15. Proposed mechanism for Knoevenagel condensation reaction catalyzed by **1-NO$_3$**.

Table S1. Knoevenagel Condensation Reaction of Benzaldehyde and Malononitrile under Different Conditions.

Entry	**1-NO_3** (mmol)	Time (h)	Temperature °C	Conversion (%)[b]
1	0	1	60	trace
2	0.001	1	60	44
3	0.002	1	60	91
4	0.003	1	60	98
5	0.004	1	60	98.6
6	0.003	1	30	17
7	0.003	1	40	66
8	0.003	1	50	85
9	0.003	1	70	98.5

Reaction conditions: benzaldehyde (1 mmol), malononitrile (2 mmol), 1 h.

Table S2. Crystallographic Data and Structural Refinement for **1-NO_3**.

Compound	**1-NO_3**
Formula	$C_{153}H_{171}N_{45}O_{54}Cd_3$
Mr	3841.54
Crystal system	hexagonal
Space group	*P* 63/mmc
a (Å)	29.1910(11)
b (Å)	29.1910(11)
c (Å)	12.9618(7)
α(°)	90.0
β(°)	90.0
γ(°)	120.0
V(Å^3)	9565.2(7)
Z	2
D_{calc} (g cm^{-3})	1.334
F(000)	3960
R_{int}	0.0921
GOF on F^2	1.031
$R_1{}^a$ [I>2σ(I)]	0.0804
$wR_2{}^b$ (all data)	0.2804

$^aR_1 = \Sigma||F_o| - |F_c||/\Sigma|F_o|$. $^bwR_2 = \{\Sigma[w(F_o^2-F_c^2)^2]/\Sigma w(F_o^2)^2]\}^{1/2}$

Table S3. Selected Bond Distances (Å) and Angles (°) for **1-NO_3**.

Cd(1)-N(3)	2.328(5)	Cd(1)-N(3)$^{\#1}$	2.328(5)
Cd(1)-N(3)$^{\#2}$	2.328(5)	Cd(1)-N(3)$^{\#3}$	2.328(5)
Cd(1)-O(2W)	2.337(11)	Cd(1)-O(1W)	2.584(7)
N(3)-Cd(1)-N(3)$^{\#1}$	177.7(2)	N(3)-Cd(1)-N(3)$^{\#2}$	95.1(2)
N(3)$^{\#1}$-Cd(1)-N(3)$^{\#2}$	84.8(2)	N(3)-Cd(1)-N(3)$^{\#3}$	84.8(2)
N(3)$^{\#1}$-Cd(1)-N(3)$^{\#3}$	95.1(2)	N(3)$^{\#2}$-Cd(1)-N(3)$^{\#3}$	177.7(2)
N(3)-Cd(1)-O(2W)	91.16(12)	N(3)$^{\#1}$-Cd(1)-O(2W)	91.16(12)
N(3)$^{\#2}$-Cd(1)-O(2W)	91.16(12)	N(3)$^{\#3}$-Cd(1)-O(2W)	91.16(12)
N(3)-Cd(1)-O(1W)	88.84(12)	N(3)$^{\#1}$-Cd(1)-O(1W)	88.84(12)
N(3)$^{\#2}$-Cd(1)-O(1W)	88.84(12)	N(3)$^{\#3}$-Cd(1)-O(1W)	88.84(12)
O(2W)-Cd(1)-O(1W)	180.0		